Pflugers Arch - Eur J Physiol (2013) 465:1281–1291
DOI 10.1007/s00424-013-1277-1

Identification of dominant negative effect of L522P mutation in the electrogenic Na^+–HCO_3^- cotransporter NBCe1

Osamu Yamazaki · Hideomi Yamada · Masashi Suzuki · Shoko Horita · Ayumi Shirai · Motonobu Nakamura · Nobuhiko Satoh · Toshiro Fujita · George Seki

Received: 6 December 2012 / Revised: 6 March 2013 / Accepted: 25 March 2013 / Published online: 5 April 2013

Abstract Homozygous mutations in the electrogenic Na^+–HCO_3^- cotransporter NBCe1 cause proximal renal tubular acidosis (pRTA) associated with extrarenal manifestations such as ocular abnormalities and migraine. Previously, the NBCe1 cytosolic mutant S982NfsX4 was shown to have a dominant negative effect by forming hetero-oligomer complexes with wild type (WT), which might be responsible for the occurrence of glaucoma and migraine in the heterozygous family members. In this study, we investigated whether the NBCe1 L522P mutant has a similar dominant negative effect. Functional analyses in *Xenopus* oocytes and HEK293 cells revealed that the L522P mutant had no transport activity due to defective membrane expression. Furthermore, when coexpressed with WT, L522P significantly reduced the transport activity of WT. In HEK293 cells, the cytosolic mutant L522P reduced the membrane expression of NBCe1 by forming hetero-oligomer complexes with WT. Among the artificial Leu^{522} mutants, L522I showed proper membrane expression and normal transport activity. However, the other mutants L522R, L522K, L522D, and L522E showed a predominant cytosolic retention. Moreover, L522R had a dominant negative effect, when coexpressed with WT. These results indicate that Leu^{522} plays an important role in the structure and trafficking of NBCe1. They also suggest that the NBCe1 mutants retaining in cytoplasm may have the dominant negative effect in common, which may induce some clinical manifestations.

Keywords NBCe1 · pRTA · ER retention · Migraine · Dominant negative effect

O. Yamazaki · H. Yamada · M. Suzuki · S. Horita · A. Shirai · M. Nakamura · N. Satoh · T. Fujita · G. Seki (✉)
Department of Internal Medicine,
The University of Tokyo, 7-3-1 Hongo,
Bunkyo-ku, Tokyo 113-0033, Japan
e-mail: georgeseki-tky@umin.ac.jp

Introduction

The electrogenic Na^+–HCO_3^- cotransporter NBCe1, encoded by *SLC4A4*, plays important roles in the regulation of extracellular and intracellular pH [28]. Three main variants of NBCe1, NBCe1A through NBCe1C, differ only at the N or C terminus [1, 28]. NBCe1A is predominantly expressed in the basolateral membranes of renal proximal tubules, where it mediates a majority of bicarbonate exit from cells [4, 28]. NBCe1B is widely expressed in several tissues including pancreatic ducts, ocular tissues, and brain, where it is involved in diverse biological processes such as pancreatic duct bicarbonate secretion, maintenance of ocular homeostasis, or regulation of synaptic pH in brain [3, 6, 23, 29, 37]. NBCe1C is predominantly expressed in brain, but its physiological roles remain speculative [2].

Homozygous inactivating mutations in NBCe1 cause proximal renal tubular acidosis (pRTA) associated with ocular abnormalities [14]. So far, 12 NBCe1 mutations have been identified in pRTA patients, corresponding to eight missense mutations R298S, S427L, T485S, G486R, R510H, L522P, A799V, and R881C, two nonsense mutations Q29X and W516X, and two frame shift mutations N721TfsX29 and S982NfsX4 as shown in Fig. 1 [7, 9, 13–16, 22, 32, 33]. Functional analyses using different expression systems indicate that at least 50 % reduction in NBCe1A activity may be required to induce severe pRTA [13, 14, 32]. Consistent with the indispensable role of NBCe1 in the systemic acid–base balance, both NBCe1 null ($NBCe1^{-/-}$) and W516X knockin ($NBCe1^{W516X/W516X}$) mice showed severe acidemia [12, 22]. Furthermore, the analysis using isolated renal proximal tubules from $NBCe1^{W516X/W516X}$ mice confirmed that bicarbonate absorption from this nephron segment is critically dependent on NBCe1 [22]. In view of widespread expression

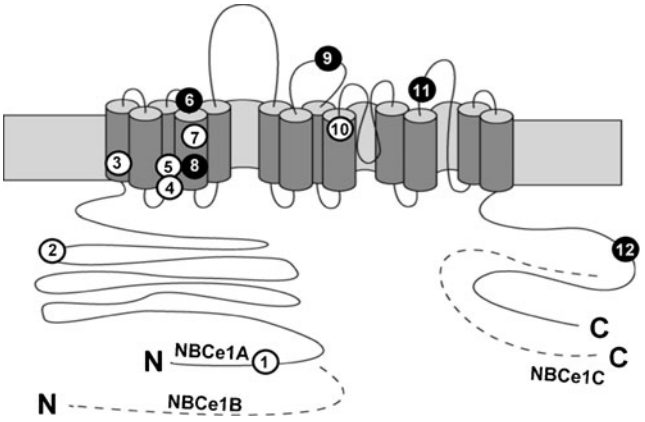

Fig. 1 Topological model of NBCe1 [39] and pRTA-related NBCe1 mutations. *Circles* show the localization of NBCe1 mutations Q29X (*1*), R298S (*2*), S427L (*3*), T485S (*4*), G486R (*5*), R510H (*6*), W516X (*7*), L522P (*8*), N721TfsX29 (*9*), A799V (*10*), R881C (*11*), and S982NfsX4 (*12*). *Black circles* indicate the association with migraine. The *dashed lines* represent the specific regions of NBCe1 variants, and the N and C denote the N and C terminus, respectively

of NBCe1 variants in the ocular tissues, the inactivation of NBCe1 activity may be directly responsible for the ocular abnormalities such as band keratopathy, cataract, and glaucoma invariably found in the pRTA patients with NBCe1 mutations [3, 37]. Several NBCe1 mutants also show trafficking defects in mammalian cells, which may cause migraine through dysregulation of synaptic pH [33].

While both of the heterozygous NBCe1-deficient mice ($NBCe1^{+/-}$ and $NBCe1^{+/W516X}$) showed mild acidemia [12, 22], pRTA has not been found in the humans heterozygous for the pathological NBCe1 mutations. Because NBCe1, like the Cl^-–HCO_3^- exchanger AE1 [8, 26], can form oligomer complexes [18]; however, some of the heterozygous NBCe1 mutations may potentially induce clinical phenotypes through a dominant negative effect especially in extrarenal tissues where the compensatory capacity for the loss of NBCe1 function may not be so efficient [22, 33, 34]. In line with this hypothesis, we have recently found that the NBCe1 S982NfsX4 mutation has a dominant negative effect by inducing the cytosolic retention of hetero-oligomer complexes of wild type (WT) and the mutant, which appears to be responsible for the occurrence of glaucoma and migraine in the heterozygous carriers of S982NfsX4 mutation [33]. However, it is unknown whether the other pRTA-related NBCe1 mutations have the similar dominant negative effect. To clarify this issue, we focused on the NBCe1 L522P mutation, which was found in a pRTA patient associated with the typical ocular abnormalities and hemiplegic migraine with episodic ataxia [7]. The L522P mutant was reported to show no transport activity due to defective trafficking in both *Xenopus* oocytes and mammalian cells [7, 32, 33].

Methods

Preparation of NBCe1 expressing constructs

cDNA encoding human NBCe1A was subcloned into pcDNA3.1/NH2-terminal GFP-TOPO or pcDNA3.1/Myc-His (both from Invitrogen), and human NBCe1B was subcloned into pcDNA3.1 as described [31, 32, 39]. The QuikChange Site-Directed Mutagenesis kit (Stratagene) was used to introduce mutations, and the complete cDNA sequence of each construct was verified by DNA sequencing.

Oocytes expression

cRNAs were transcribed from the appropriately linearized NBCe1A templates with the mMESSAGE mMACHINE high-yield Capped RNA Transcription kit (Ambion). Oocytes were removed from *Xenopus laevis*, dissociated with collagenase as described [13, 31, 32] and were injected with varying doses of cRNA expressing GFP-tagged WT (GFP-WT) and/or the GFP-tagged L522P mutant (GFP-L522P) in a total volume of 50 nl. Electrophysiological studies were performed 3–5 days after cRNA injection.

Electrophysiological analysis in oocytes

Nominally HCO_3^--free ND96 solution contained (in millimolars) 96 NaCl, 2 KCl, 1 $MgCl_2$, 1.8 $CaCl_2$, and 5 mM 4-(2-hydroxyethyl)-1-piperazine ethanesulphonic acid (HEPES) at a pH of 7.4. HCO_3^--containing solution was prepared by replacing 30 mM NaCl with 30 mM $NaHCO_3$ in ND96, and was equilibrated with 5 % CO_2 in oxygen (pH 7.4). Electrophysiological studies were performed as described but slightly modified [13, 31, 32, 39]. In brief, an oocyte was placed in a perfusion chamber and superfused with ND96 solution at a rate of ~4 ml/min, and a two-electrode voltage clamp method was used with a model OC-725C oocyte clamp (Warner Instruments), controlled by the Clampex module of pCLAMP software (Axon Instruments). We monitored the NBCe1A currents induced by solution changes from ND96 to HCO_3^--containing solution at a holding potential of −25 mV, because the baseline current was minimal at this voltage when oocytes were bathed in ND96 solution [13, 32, 39]. Solution changes from ND96 to HCO_3^--containing solution did not induce any currents in oocytes injected with H_2O as described [13, 32, 39].

Expression in cultured cells

MDCK and HEK293 cells were grown on culture dishes in Dulbecco's modified Eagle's medium supplemented with 10 % fetal calf serum. These cells were transfected with plasmid expressing each NBCe1 construct with LipofectAMINE 2000 (Invitrogen). The same amounts of DNA (3 μg/well of 6-well

dishes or 18 μg/dish of 10-cm dishes) were transfected for the WT NBCe1 and the mutants. For coexpression, the total amounts of DNA were kept constant (6 μg/well of 6-well dishes or 36 μg/dish of 10-cm dishes) by adding empty vector, if necessary. We performed cell pH measurement, immunoblotting, or immunofluorescence analysis 48 h after transfection.

Cell pH measurement

HEPES-buffered solution contained (in millimolars) 127 NaCl, 5 KCl, 1.5 $CaCl_2$, 1 $MgCl_2$, 2 NaH_2PO_4, 1 Na_2SO_4, 25 HEPES, and 5.5 glucose; adjusted to pH 7.4 by 1 N NaOH. HCO_3^--Ringer solution contained (in millimolars) 115 NaCl, 5 KCl, 1.5 $CaCl_2$, 1 $MgCl_2$, 2 NaH_2PO_4, 1 Na_2SO_4, 25 $NaHCO_3$, and 5.5 glucose; pH 7.4 equilibrated with 5 % CO_2/95 % O_2 gas. Na^+ was replaced by *N*-methyl-D-glucamine in Na^+-free HCO_3^- solution. HEK293 cells were grown on fibronectin-coated coverslips. Two days after transfection, cells were incubated with the pH dye acetoxymethylester of bis(carboxyethyl)carboxyfluorescein (BCECF/AM; Molecular Probes). Cell pH was measured with a microscopic fluorescence photometry system (OSP-10; Olympus) as described [13, 32, 33, 39]. The intracellular BCECF dye was alternatively excited at two wavelengths (440 and 490 nm), and emission was measured at a wavelength of 530 nm. NBCe1A activity in HEK293 cells was analyzed by monitoring Na^+- and HCO_3^--dependent cell pH recovery as described [33, 39]. Cells were first superfused with HEPES-buffered solution. Solution was exchanged to Na^+-free HCO_3^--solution, which induced a marked intracellular acidification due to CO_2 entry and reversal of the endogenous Na^+/H^+ exchangers (NHEs). Thereafter, solution was exchanged to HCO_3^--Ringer solution containing 1 mM amiloride, which blocks the endogenous NHEs activity. The resultant Na^+- and HCO_3^--dependent cell pH recovery (dpH_i/dt) represents the NBCe1A activity [33, 39]. Some cells transfected with vector alone or the nonfunctional NBCe1 mutant such as L522P showed a gradual intracellular acidification even after solution was exchanged to HCO_3^--Ringer solution containing 1 mM amiloride. We do not know the underlying mechanism of this phenomenon at present. The intrinsic cell buffer capacity (β_i) was measured with the NH_4Cl pulse method as described [13, 39]. Total cell buffer capacity (β_T) in the HCO_3^--containing solution was equal to the sum of β_i and the HCO_3^- buffer capacity ($\beta_{HCO_3^-}$), and the HCO_3^- flux through NBCe1A was calculated as $dpH_i/dt \times \beta_T$ as reported [39].

Immunoblotting, immunoprecipitation, and cell surface biotinylation

Whole oocytes extracts were obtained according to the method previously described [16]. In brief, groups of 20 oocytes were homogenized in ice-cold hypotonic buffer (in millimolars: 7.5 potassium phosphate, pH 7.4, 1 EDTA, 1 phenylmethyl sulphonyl fluoride (PMSF), 1 μg/ml pepstatin A, and 1 μg/ml leupeptin). The homogenate was centrifuged twice at 1,000×*g* for 10 min to remove yolk granules and cellular debris. The obtained samples were dissolved in a sample-loading buffer containing 2 % SDS and were subjected to Western blotting with an anti-GFP antibody (Clontech).

For immunoprecipitation, HEK293 cells, grown on a 10-cm culture dish, were cotransfected with Myc-tagged WT (Myc-WT) and GFP-L522P. After 48 h, the cells were lysed with a lysis buffer containing 50 mM Tris/pH 8.0, 150 mM NaCl, 1 % Nonidet P-40, 0.5 % sodium deoxycholate, 0.1 % SDS, and 1 mM PMSF. The cell lysate was precleaned by incubation with Protein G Sepharose 4 Fast Flow (GE Healthcare Bio-Science) and incubated with an anti-Myc (Bethyl Laboratories) or the anti-GFP antibody coupled to Protein G Sepharose 4 Fast Flow. The immunoprecipitates were washed three to five times with lysis buffer and subjected to Western blotting as described [33]. Cell surface biotinylation in HEK293 cells was performed with the Pierce Cell Surface Protein Isolation Kit (Thermo Scientific) according to the manufacturer's protocol. In brief, cells, grown on 10-cm culture dishes, were washed with phosphate-buffered solution (PBS), incubated with EZ-LINK Sulfo-NHS-SS-biotin for 30 min at 4 °C followed by the addition of a quenching solution. Cells were lysed with lysis buffer (500 μl) containing the Halt protease inhibitor cocktail kit. An aliquot (100 μl) of the lysate (total) was saved for Western blotting. The biotinylated NBCe1 was isolated with NeutrAvidin agarose gel, eluted by the sample buffer (400 μl) containing dithiothreitol, and subjected to Western blotting with the anti-GFP or anti-Na/K pump α1 antibody (Upstate Biotech) as described [33, 39].

For deglycosylation study, the protein samples were heat denatured at 70 °C for 10 min, and then incubated overnight at 37 °C in the presence of 5 U/ml *N*-glycosidase F (Roche) according to the manufacturer's instructions as described [38].

Immunofluorescence

HEK293 cells or confluent MDCK cells were grown on fibronectin-coated coverslips. We used the confluent MDCK cells on coverslips, because they were shown to retain the proper cell polarity, as evidenced by the basolateral distribution of Na/K pump and the formation of tight junctions [32, 36]. Indeed, these MDCK cells showed the proper ZO-1 staining [32]. Moreover, the expression of NBCe1 was shown to be more efficient in this condition than when they were grown on permeable supports [36]. The cells were fixed in 4 % paraformaldehyde in PBS, permeabilized with 0.1 % Triton X-100 (Sigma) in PBS, stained with the F-actin dye tetramethylrhodamine isothiocyanate-phalloidin (Sigma) or phalloidin CruzFluor 633 conjugate (Santa Curz), and observed by a TCS SL

laser-scanning confocal microscope (Leica) as described [32, 33, 39]. To visualize Myc-NBCe1A, a rabbit polyclonal anti-Myc (Bethyl Laboratories) or a mouse monoclonal anti-Myc (Wako) was used as the primary antibody. To visualize the endoplasmic reticulum (ER), a rabbit polyclonal anti-protein disulfide isomerase PDI (Stressgen Bioreagents) was used as the primary antibody. To visualize NBCe1B, a rabbit polyclonal antibody against the NBCe1B-specific N terminal region, which does not recognize NBCe1A [37], was used. Alexa Fluor 546 goat anti-rabbit IgG or Alexa Fluor 488 goat anti-mouse IgG (both from Molecular Probes) was used as the secondary antibody as described [33].

Statistic analysis

The data were represented as mean ± SEM. Significant differences were determined by applying Student's *t* test or ANOVA with Bonferroni's correction, as appropriate. Statistical significance was set at $p<0.05$.

Results

Functional analysis in *Xenopus* oocytes

To examine whether the NBCe1 L522P mutation has a dominant negative effect, we first performed functional analysis in *Xenopus* oocytes, which have been used to characterize the functional properties of NBCe1 [9, 13, 27, 28, 33, 36, 39]. The outward currents induced by the solution exchange from ND96 solution to HCO_3^--containing solution at a holding potential of −25 mV were used to determine the NBCe1A activities as reported [13, 31–33, 39]. As shown in Fig. 2a, oocytes injected with WT-NBCe1A showed large NBCe1 currents. By contrast, the L522P mutant had no electrogenic activities presumably due to the lack of expression in the oocyte membrane as reported [7]. Furthermore, the coexpression of L522P significantly inhibited the WT currents. These data suggest that L522P has a dominant negative effect. As shown in Fig. 2b, Western blotting analysis of whole oocytes extracts revealed the similar expression levels of WT and L522P. Compared with WT, however, the L522P mutant showed the lower band, which might represent the immature or only partially glycosylated forms of NBCe1 (see below).

Intracellular expression in mammalian cells

To clarify the dominant negative effect of L522P in more detail, we next examined the intracellular expression in MDCK cells, which are suitable for the examination of trafficking behaviors of NBCe1 mutants in the polarized epithelia [19, 32, 33, 36]. As shown in Fig. 3a, GFP-WT-NBCe1A was predominantly localized to the basolateral membranes. By contrast, GFP-L522P showed a predominant cytosolic retention as reported [32]. As shown in Fig. 3b, GFP-L522P showed a predominant cytosolic retention also in HEK293 cells. Moreover, the cytosolic expression of L522P was largely overlapped with the ER marker PDI, indicating that the mutant was mostly retained in the ER. The similar overlapping with PDI as shown in Fig. 3c indicated that GFP-L522P was mostly retained in the ER also in MDCK cells.

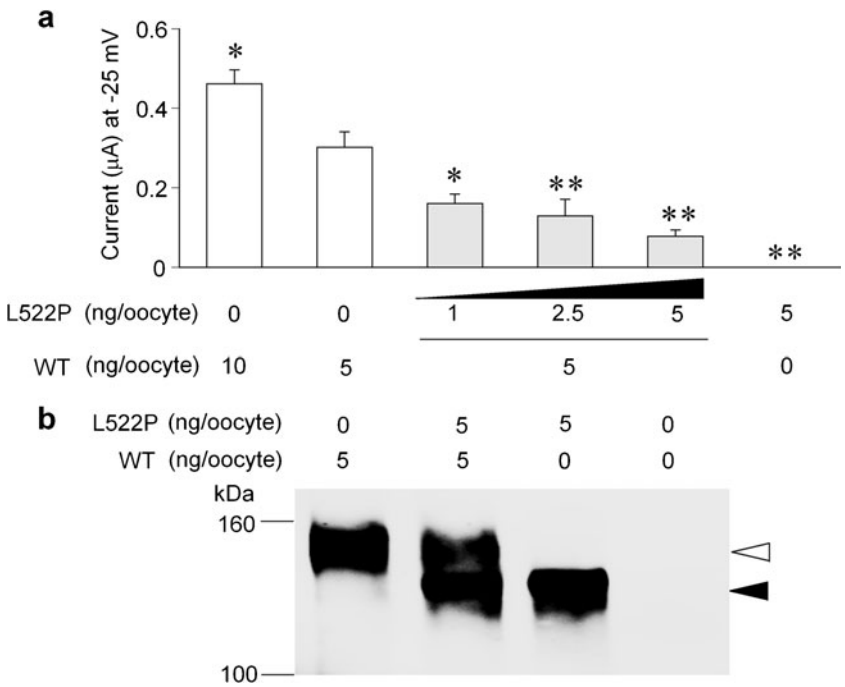

Fig. 2 Functional analysis in *Xenopus* oocytes. **a** Oocytes were injected with WT and/or L522P cRNA at the indicated amounts, and NBCe1 currents were elicited by solution change from ND96 solution to HCO_3^- containing solution. *$p<0.05$ vs. WT (5 ng); **$p<0.01$ vs. WT (5 ng). Numbers of observation are 7–10 for each experiment. **b** Western blotting analysis of whole oocytes extracts. WT predominantly showed the higher band (*open triangle*), while the L522P mutant showed the lower band (*closed triangle*)

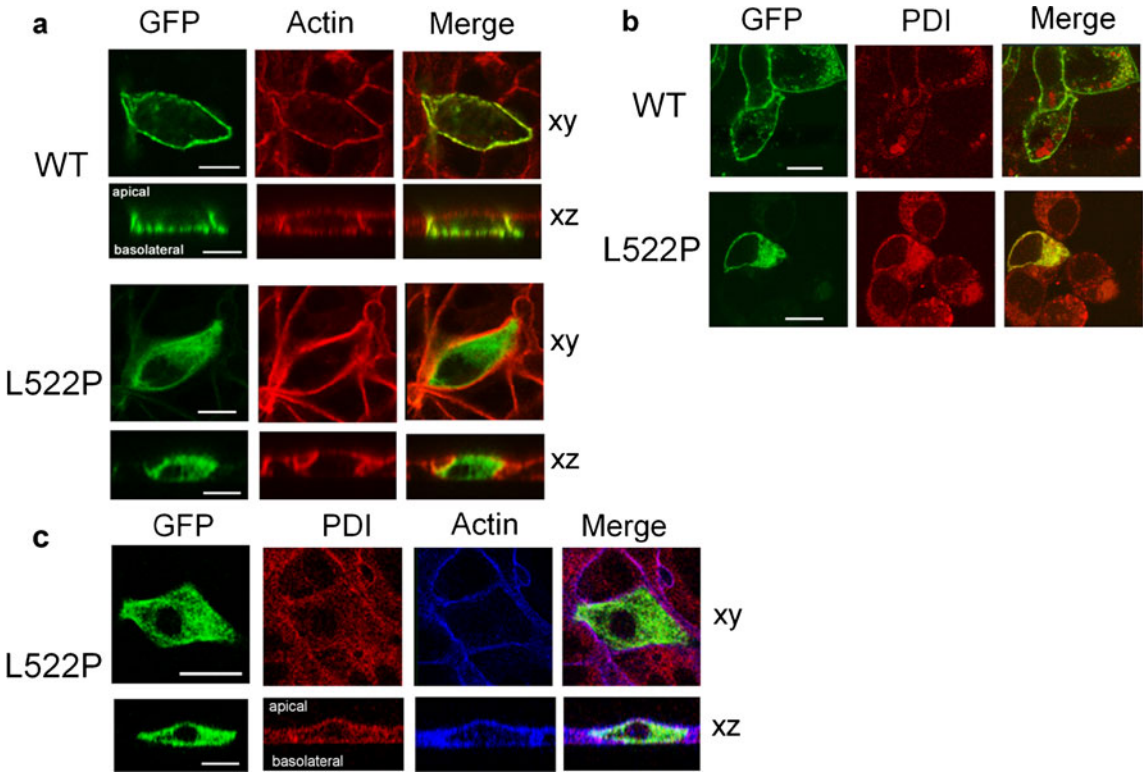

Fig. 3 Immunological localization of WT and L522P in mammalian cells. **a** Expression of GFP-WT and GFP-L522P in MDCK cells. NBCe1 is shown in *green*, and actin in *red*. *xy* indicates front view, and *xz* side view. *Bars* indicate 10 μm. **b** Expression in HEK293 cells. Note that GFP-L522P largely colocalized with the ER marker PDI (*red*). *Bars* indicate 10 μm. **c** Localization of L522P in MDCK cells. NBCe1 is shown in *green*, PDI in *red*, and actin in *blue*. *Bars* indicate 10 μm

Association of WT and L522P

To examine a possible interaction between WT-NBCe1A and the L522P mutant, we expressed Myc-WT together with GFP-WT or GFP-L522P in HEK293 cells. As shown in Fig. 4a, the Myc-WT and GFP-WT signals predominantly colocalized at the plasma membrane. By contrast, the Myc-WT and GFP-L522P signals predominantly colocalized in the cytoplasmic region, supporting the dominant negative effect of L522P by forming the hetero-oligomer complexes with WT. We next examined the interaction between WT and the L522P mutant by a coimmunoprecipitation assay. We expressed Myc-WT together with GFP-L522P in HEK293 cells, and cell lysates were subjected to immunoprecipitation with an anti-Myc or an anti-GFP antibody. Consistent with the oligomer formation of NBCe1 [18, 33], we confirmed the interaction between WT and L522P as shown in Fig. 4b.

Functional analysis in HEK293 cells

To quantitate the dominant negative effect of L522P, we expressed WT-NBCe1A and/or the L522P mutant in HEK293 cells, and performed functional analysis as reported [33, 39]. While WT induced a robust Na^+- and HCO_3^--dependent cell pH recovery reflecting the NBCe1 activity [33, 39], the L522P mutant induced no NBCe1 activity as shown in Fig. 5a. As summarized in Fig. 5b, the coexpression of WT and L522P significantly reduced the net NBCe1 activity, directly confirming the dominant negative effect of L522P. As shown in Fig. 5c, biotinylation Western blotting revealed the reduction in biotinylated NBCe1 by the coexpression of WT and L522P. In Western blotting of the total fractions, WT showed the predominant higher molecular band and the faint lower molecular band while L522P showed only the lower band. The deglycosylation study in Fig. 5d confirmed that the lower-molecular band represents the immature or only partially glycosylated forms of NBCe1 that retain in cytosolic compartments [5]. These results support a view that the reduction in surface expression of NBCe1 due to the cytosolic formation of hetero-oligomer complexes with WT is responsible for the dominant negative effect of L522P.

Characterization of other Leu^{522} mutations

Previously, Zhu et al. examined the topological location and structural importance of NBCe1 residues by the substituted

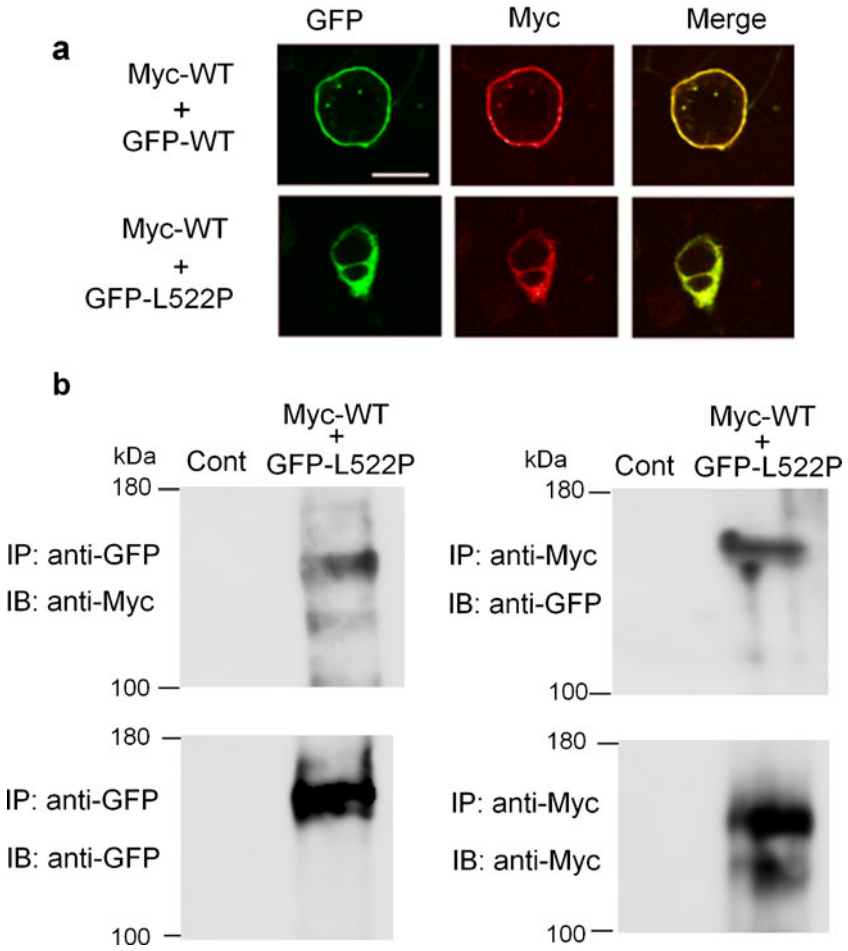

Fig. 4 Interaction between WT and L522P. **a** Coexpression of Myc-WT (*red*) together with GFP-WT or GFP-L522P in HEK293 cells. *Bar* indicates 10 μm. **b** Immunoprecipitation with anti-Myc or anti-GFP antibody in HEK 293 cells coexpressed with Myc-WT and GFP-L522P. Cont: vector-transfected control cells

cysteine accessibility method [40]. Because L522C did not impair membrane processing and showed a significant transport activity corresponding to approximately 70 % of the WT activity, they proposed that it is the proline residue rather than the loss of leucine that causes intracellular retention of NBCe1 [40]. To further clarify the roles of Leu^{522} in the trafficking and function of NBCe1, we introduced several artificial Leu^{522} mutations into the GFP-WT-NBCe1A construct.

Functional analysis in HEK293 cells revealed that the introduction of a subtle structural modification (L522I) did not affect the transport activity of NBCe1 as shown in Fig. 6a. However, the introduction of both basic (L522R and L522K) and acidic (L522D and L522E) residues markedly reduced the transport activity corresponding to 13–27 % of the WT activity. Biotinylation Western blotting in Fig. 6b confirmed that while L522I showed a similar level of membrane expression as WT, the other mutants L522R, L522K, L522D, and L522E showed markedly reduced levels of membrane expression. Western blotting of the total fractions revealed that while the L522I predominantly yielded the mature form of NBCe1, the other mutants yielded the substantial amounts of immature forms of NBCe1. We next examined the intracellular localization of these mutants in HEK293 cells as shown in Fig. 6c. While L522I showed a predominant membrane expression, all the other mutants L522R, L522K, L522D and L522E showed a similar cytosolic retention. We also examined the intracellular localization in MDCK cells as shown in Fig. 6d. The L522I showed a predominant basolateral expression that was indistinguishable from that of WT-NBCe1A. By contrast, all the other mutants showed a predominant cytosolic retention.

We next performed the coexpression analysis of WT together with L522I or L522R in HEK293 cells. As shown in Fig. 7a, the transport activity obtained by the coexpression of WT and L522I was rather higher than that of WT alone. However, the transport activity by the coexpression of WT and L522R was significantly lower than that of WT alone, indicating that the L522R mutant has a dominant negative effect. Biotinylation Western blotting in Fig. 7b confirmed that the surface expression of NBCe1A was increased by the coexpression of WT and L522I but was decreased by the coexpression of WT and L522R. Western blotting of the total fractions confirmed the definite intracellular expression of L522R. To examine the nature of dominant negative effect of L522R, we coexpressed Myc-WT together with GFP-L522I or GFP-L522R in HEK293 cells. As shown in Fig. 7c, the Myc-

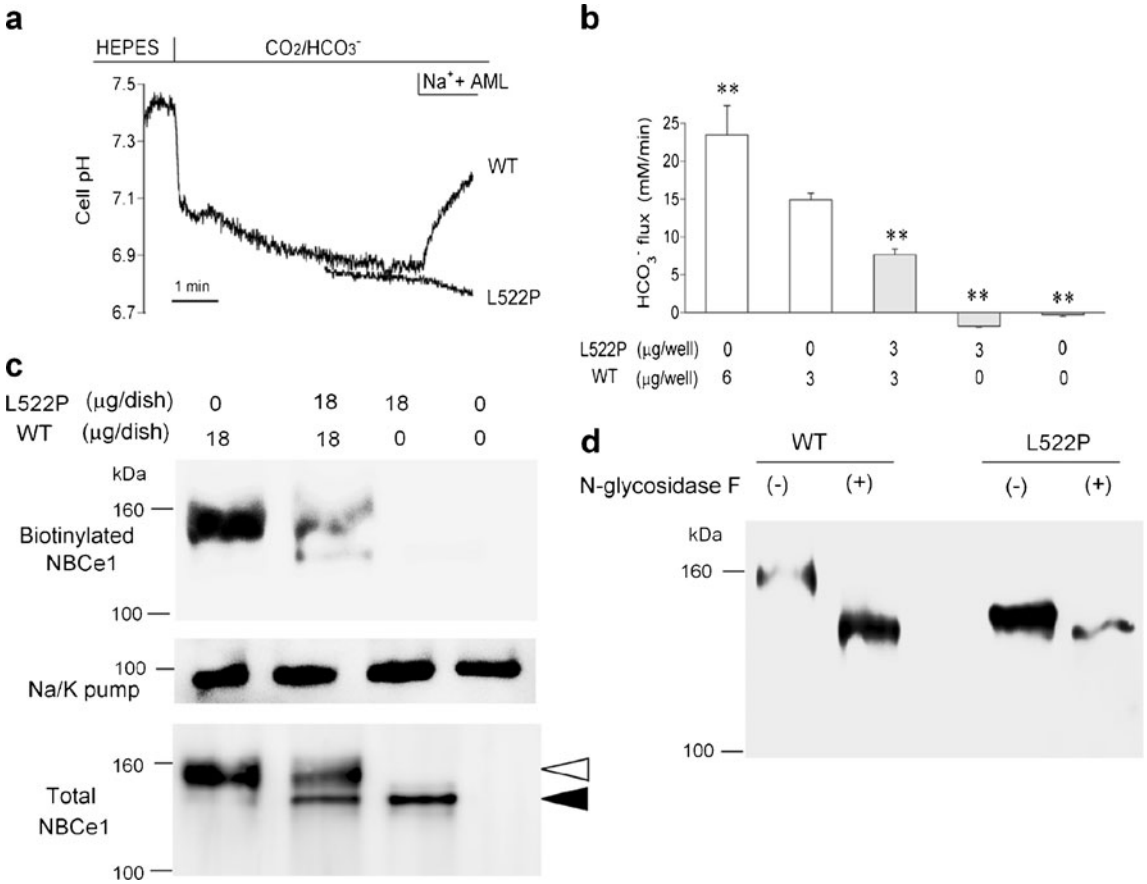

Fig. 5 Functional analysis in HEK293 cells. **a** Original traces from cells transfected with WT or L522P. Only WT showed Na^+- and HCO_3^--dependent cell pH recovery, corresponding to NBCe1 activity. *AML* amiloride. **b** Summary data for NBCe1-mediated HCO_3^- fluxes. Cells seeded in 6-well dishes were transfected with WT and/or L522P cDNA at the indicated amounts. $^{**}p<0.01$ vs. WT (3 μg). Numbers of observation are 9–25 for each experiment. **c** Cell surface expression of NBCe1. Cells seeded in 10-cm dishes were transfected with WT and/or L522P cDNA at the indicated amounts. Blots with the anti-GFP antibody in biotinylated (3 μl/lane) and total fractions (15 μl/lane) are shown. Equal protein loading in biotinylated fractions is confirmed by blots with the anti-Na/K pump. In total fractions, WT predominantly showed the higher band (*open triangle*), while L522P showed the lower band (*closed triangle*). A representative blot from three independent experiments is shown. **d** The deglycosylation study using the total fractions with or without *N*-glycosidase F treatment

WT and GFP-L522I signals predominantly colocalized at the plasma membrane. By contrast, the Myc-WT and GFP-L522R signals predominantly colocalized in the cytosolic region, indicating that the nature of dominant negative effect of L522R is similar to that of L522P.

Intracellular association between NBCe1 constructs without GFP tag

Because the addition of a large molecule such as GFP into N-terminal may potentially influence the association between NBCe1 constructs, we finally performed the coexpression analysis in HEK293 cells using the NBCe1 constructs without GFP tag. To achieve this end, we used Myc-NBCe1A-WT and the untagged NBCe1B constructs NBCe1B-WT or NBCe1B-L566P (the NBCe1B version of NBCe1A-L522P). As shown in Fig. 8a, we first confirmed the specificity of the mouse anti-Myc antibody and the rabbit anti-NBCe1B antibody. We then coexpressed Myc-NBCe1A-WT together with NBCe1B-WT or NBCe1B-L566P. As shown in Fig. 8b, Myc-NBCe1A-WT and NBCe1B-WT predominantly colocalized at the plasma membrane. By contrast, the Myc-NBCe1A-WT and NBCe1B-L566P signals predominantly colocalized in the cytosolic region. These results indicate that the addition of GFP does not significantly modify the association between NBCe1 constructs. The apparent intracellular association between NBCe1A and NBCe1B constructs is also consistent with a previous study suggesting that N- or C-terminal cytoplasmic structures may not be essential for the oligomerization of NBCe1 [11].

Discussion

We previously identified that the NBCe1 S982NfsX4 mutant can reduce the plasma membrane expression of NBCe1 by forming the cytosolic hetero-oligomer complexes with

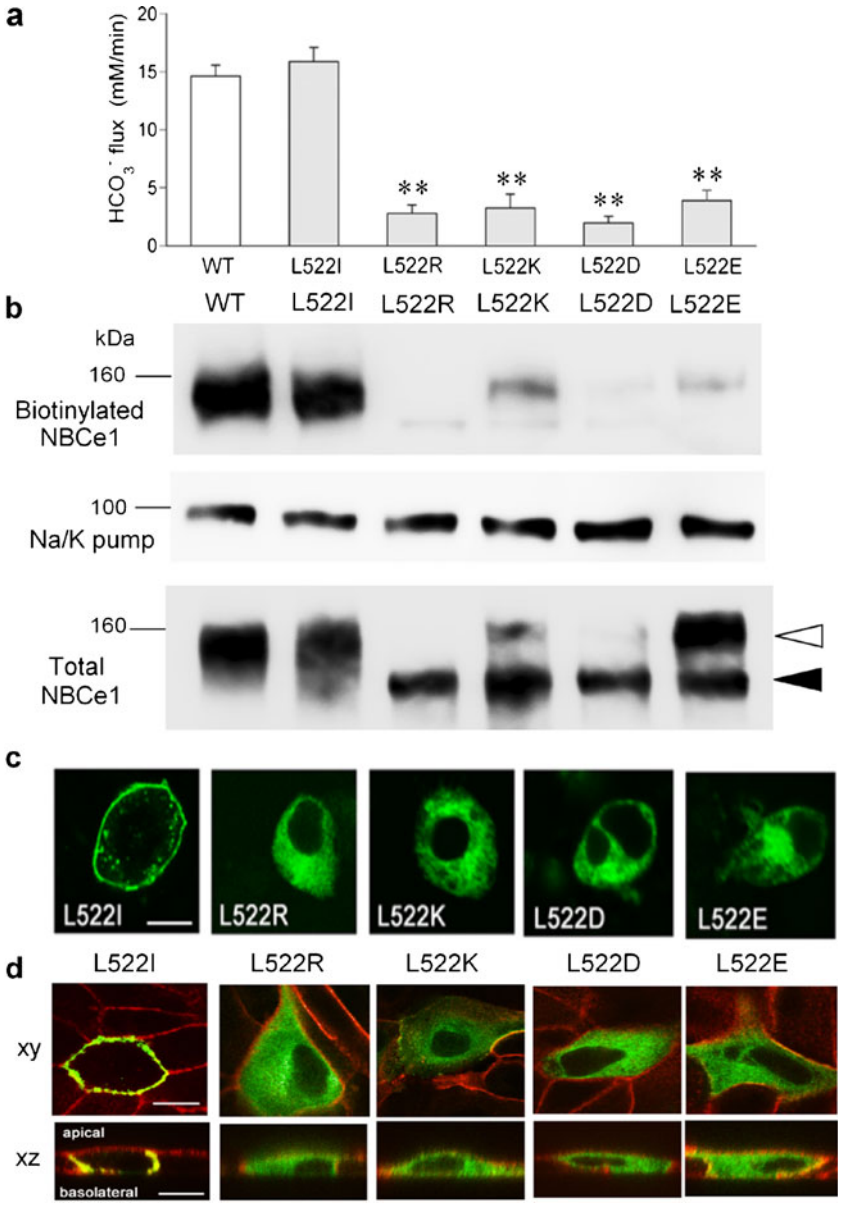

Fig. 6 Characterization of artificial Leu^{522} mutants. **a** Summary data for NBCe1-mediated HCO_3^- fluxes in cells transfected with WT or mutants (each cDNA at 3 μg/well). $^{**}p < 0.01$ vs. WT. Numbers of observation are 6–13 for each experiment. **b** Cell surface expression of NBCe1 and Na/K pump. Cells seeded in 10-cm dishes were transfected with 18 μg of each construct. In Western blotting of total fractions, the higher band (*open triangle*) represented the mature form of NBCe1, while the lower band (*closed triangle*) represented the immature forms of NBCe1. A representative blot from three independent experiments is shown. **c** Intracellular localization in HEK293 cells. *Bar* indicates 10 μm. **d** Intracellular localization in MDCK cells. NBCe1 is shown in *green*, and actin in *red*. *xy* indicates front view, and *xz* side view. *Bars* indicate 10 μm

WT [33]. The present study revealed that the L522P mutant, which showed the predominant cytosolic retention in both *Xenopus* oocytes and mammalian cell, had the similar dominant negative effect. We also found that the introduction of other artificial mutations such as L522R, L522K, L522D, and L522E, but not L522I caused the cytosolic retention in HEK293 cells, among which we confirmed the dominant negative effect of L522R. These results suggest that the NBCe1 mutants retaining in the cytosolic regions may have the dominant negative effect in common.

The bicarbonate absorption from renal proximal tubules is critically dependent on the NBCe1 activity, and Na^+-independent and Na^+-dependent Cl^-–HCO_3^- exchangers, also known to exist in the basolateral membrane of this nephron segment [25], cannot effectively compensate for the reduction of NBCe1 activity [22]. Instead, proton secretion from renal distal tubules can at least partially compensate for the substantial reduction of bicarbonate absorption from proximal tubules, and this compensatory ability of distal tubular acidification may be higher in humans than in mice [22]. Indeed, acidemia has not been reported in the pRTA family members carrying the heterozygous NBCe1 mutations. On the other hand, the compensatory capacity for the loss of NBCe1 activity may not be so efficient in the other tissues. For example, NBCe1 in astrocytes may play an important role in the regulation of synaptic pH in the brain [6]. In particular, the net extracellular acidosis due to depolarization-induced alkalinization (DIA) usually makes surrounding neuronal cells less excitable, because extracellular protons in the physiological range of pH can block the excitatory NMDA receptors [6]. Importantly, astrocytes from $NBCe1^{-/-}$ mice do not show DIA,

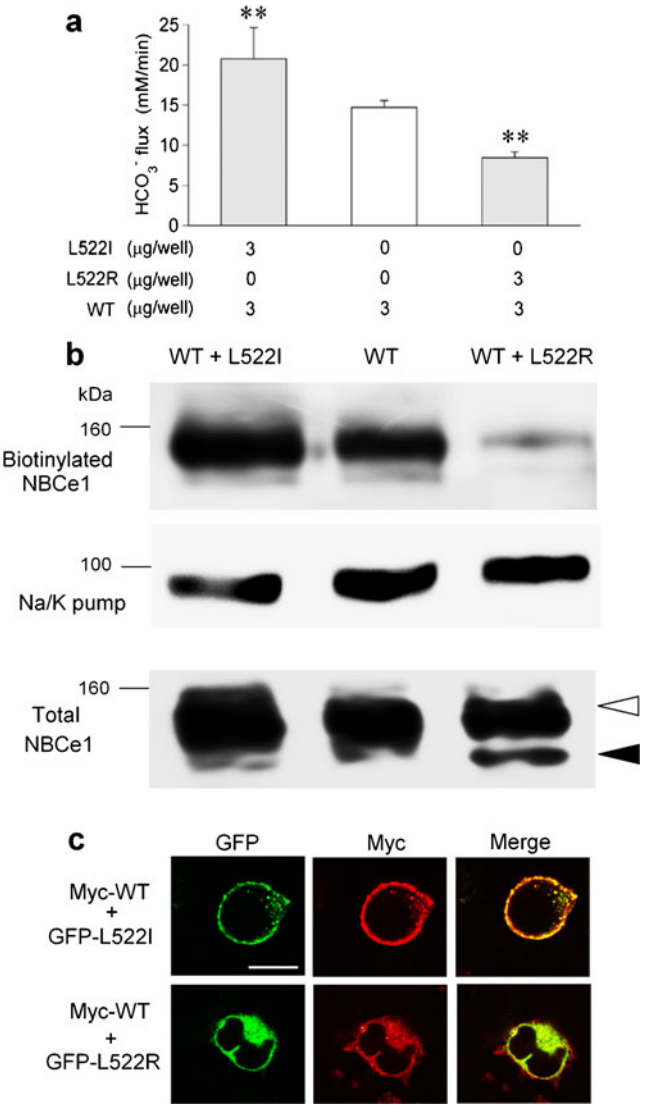

Fig. 7 Interaction between WT and L522I or L522R. **a** Summary data for NBCe1-mediated HCO_3^- fluxes in cells transfected with WT and L522I or L522R cDNAs at the indicated amounts. $^{**}p<0.01$ vs. WT alone. Numbers of observation are 9–11 for each experiment. **b** Cell surface expression of NBCe1 and Na/K pump. Cells seeded in 10-cm dishes were transfected with 18 μg of WT together with 18 μg of L522I, vector, or L522R. Western blotting of total fractions confirmed the expression of both mature (WT and L522I) and immature forms (L522R) of NBCe1. A representative blot from three independent experiments is shown. **c** Coexpression of Myc-WT (*red*) together with GFP-L522I or GFP-L522R in HEK293 cells. *Bar* indicates 10 μm

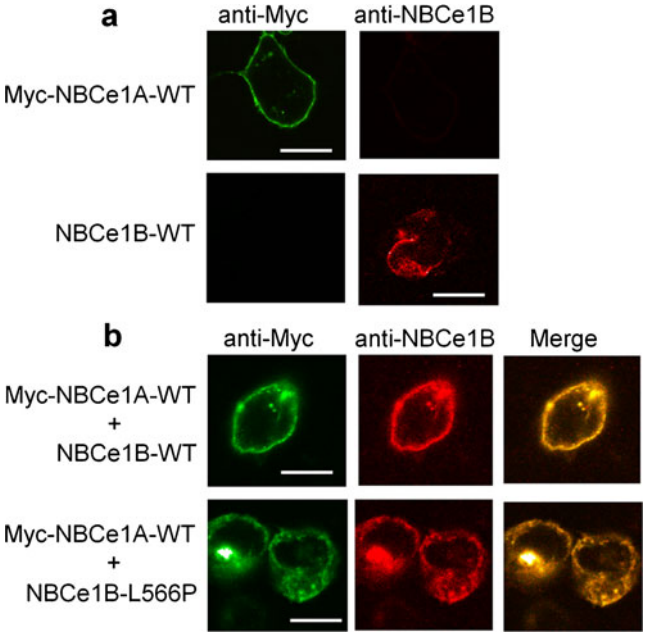

Fig. 8 Intracellular expression of NBCe1 constructs without GFP tag. **a** Expression of Myc-NBCe1-WT or NBCe1B-WT. Cells were transfected with each construct and treated with anti-Myc (*green*) and anti-NBCe1B (*red*) antibodies. *Bars* indicate 10 μm. **b** Coexpression of Myc-NBCe1A-WT together with NBCe1B-WT or NBCe1B-L566P. *Bars* indicate 10 μm

suggesting that the other acid/base transporters in astrocytes cannot compensate for the pH regulatory role of NBCe1 [34]. Thus, the absence of DIA due to the loss of NBCe1 activity may cause a positive feedback loop of increased neuronal activity leading to further NMDA-mediated neuronal hyperactivity, resulting in cortical spreading depression and migraine aura [33]. The mechanism of glaucoma due to NBCe1 mutations is less clear. In case of high-tension glaucoma usually found in the pRTA patients carrying the homozygous NBCe1 mutations, NBCe1 in trabecular meshwork cells may play a key role by controlling the aqueous humor outflow [37]. In case of normal-tension glaucoma identified in the family members carrying the heterozygous NBCe1 mutation [33], NBCe1 in retinal Müller cells seems to play an important role by counteracting the potentially toxic effects of light-induced extracellular alkalosis [3, 24]. Consistent with rather insufficient compensatory capacities in these extrarenal tissues, the family members carrying the heterozygous S982NfsX4 mutation were found to have migraine and normal-tension glaucoma [33].

Most of the pRTA patients with homozygous NBCe1 mutations are of short stature [7, 9, 13–16, 32], which may be caused by the suppressive effect of chronic acidemia on bone matrix mineralization [10]. Indeed, these patients usually have severe acidemia with blood HCO_3^- concentrations of less than 13 mM [9, 13–16, 32], and alkali therapy, if started early in life, can at least partially improve bone formation in the human pRTA patient [30] as well as the $NBCe1^{W516X/W516X}$ mice [22]. Although the S982NfsX4 mutant showed a predominant cytosolic retention in mammalian cells, it showed a normal transport activity in *Xenopus* oocytes [33]. Interestingly, both of the two sisters carrying the homozygous S982NfsX4 mutation, who showed relatively mild acidemia with blood HCO_3^- concentrations of 14.8 and 17.3 mM, respectively, were of normal stature [33]. Probably, a small amount of the S982NfsX4

mutant may escape from ER retention and reach the plasma membrane in vivo, thereby preventing the complete loss of NBCe1 activity from renal proximal tubules. While the blood bicarbonate concentrations of the patient carrying the homozygous L522P mutation were not reported, his definitely short stature corresponding to about tenth percentile for age strongly suggests the presence of severe acidemia [7]. Furthermore, unlike the S982NfsX4 mutant, the L522P showed no transport activity in both *Xenopus* oocytes and HEK293 cells. From these considerations, it is not unreasonable to speculate that the dominant negative effect of L522P may also lead to some clinical phenotypes. Besides the potential occurrence of migraine and glaucoma, the heterozygous L522P carriers could have low blood pressure due to defective Na^+ absorption from renal proximal tubules. Indeed, rare heterozygous mutations in renal salt handling genes such as *SCL12A3*, *SLC12A1*, and *KCNJ1* have been shown to result in the lower blood pressure [17]. Unfortunately, however, we cannot get any information about the effects of the heterozygous L522P mutation on human health, because the pRTA patient carrying the homozygous L522P mutation was adopted at age 4 months [7]. In addition, single nucleotide polymorphisms in Leu^{522} have not been identified at present (http://www.ncbi.nlm.nih.gov/projects/SNP/snp_ref.cgi?chooseRs=coding&go=Go&locusId=8671).

NBCe1 may have 13–14 transmembrane segments (TMs), and Leu^{522} locates in TM 4. The previous study with the substituted cysteine accessibility method by Zhu et al. [40] revealed that Leu^{522}, like the other pRTA-related NBCe1 residues, may be buried deep in the protein complex/lipid bilayer but not line the ion translocation pore. Because L522C was found to show the proper membrane expression, they proposed that the introduction of major structural change by the proline residue was responsible for the cytosolic retention [40]. The present study, however, revealed that the introduction of both positive (L522R and L522K) and negative (L522D and L522E) charge residues induced the cytosolic retention, suggesting that Leu^{522} plays a pivotal role in the structure and trafficking of NBCe1. Mutations in the critical Leu^{522} residue may induce significant changes in the local structure of NBCe1 prerequisite for the protein quality control in the ER. Because the crystal structures of NBCe1 transmembrane domains have not been obtained, it is rather difficult to specify the effects of individual Leu^{522} mutations on the local structure of NBCe1. We cannot entirely exclude the specific effect of proline residue, however, because unlike the L522P mutant completely lacking the transport activity, the other cytosolic mutants L522R, L522K, L522D, and L522E showed small residual transport activities. Previous studies identified the two cytosolic motifs potentially important for the proper trafficking of NBCe1: the $Phe^{1023}Leu^{1014}$ signal in the C-terminal region, which may be essential for the basolateral targeting [20], and the Asp^{405} and Asp^{416} residues in the N-terminal region [21], which may be required for the binding of adaptor proteins such as protein 4.1B [35]. Interestingly, the artificial mutants F1013L, D405A, and D416A, which displayed a predominant cytosolic retention in mammalian cells, still showed some residual electrogenic activities in *Xenopus* oocytes [20, 21]. Similarly, the pRTA-related mutant R881C also displayed a predominant cytosolic retention in mammalian cells but still showed a modest electrogenic activity in *Xenopus* oocytes [13, 33, 36]. It is therefore possible that the L522P mutation may severely disrupt a scaffolding helix in TM4 that is important for the second stage folding of NBCe1 as previously suggested [40].

In summary, we identified that the pRTA-related NBCe1 mutation L522P has the dominant negative effect by forming hetero-oligomer complexes with WT. Leu^{522} seems to be quite important for the structure and trafficking of NBCe1, because the introduction of both positive and negative charge residues induced the cytosolic retention. Functional analyses suggested, however, that the L522P mutation might disrupt the local folding structure of NBCe1 more severely than the other artificial Leu^{522} mutations.

Acknowledgments This work was supported in part by grants from the Ministry of Education, Culture, Sports, Science and Technology of Japan (H.Y. and G. S.) and by the 2012 Research Grant of the 60th Anniversary Memorial Fund from Nihon University Medical Alumni Association (O.Y.).

References

1. Abuladze N, Song M, Pushkin A, Newman D, Lee I, Nicholas S, Kurtz I (2000) Structural organization of the human NBC1 gene: kNBC1 is transcribed from an alternative promoter in intron 3. Gene 251:109–122
2. Bevensee MO, Schmitt BM, Choi I, Romero MF, Boron WF (2000) An electrogenic Na^+–HCO_3^- cotransporter (NBC) with a novel COOH-terminus, cloned from rat brain. Am J Physiol Cell Physiol 278:C1200–C1211
3. Bok D, Schibler MJ, Pushkin A, Sassani P, Abuladze N, Naser Z, Kurtz I (2001) Immunolocalization of electrogenic sodium-bicarbonate cotransporters pNBC1 and kNBC1 in the rat eye. Am J Physiol Renal Physiol 281:F920–F935
4. Boron WF (2006) Acid–base transport by the renal proximal tubule. J Am Soc Nephrol 17:2368–2382
5. Chen LM, Qin X, Moss FJ, Liu Y, Boron WF (2012) Effect of simultaneously replacing putative TM6 and TM12 of human NBCe1-A with those from NBCn1 on surface abundance in *Xenopus* oocytes. J Membr Biol 245:131–140
6. Chesler M (2003) Regulation and modulation of pH in the brain. Physiol Rev 83:1183–1221
7. Demirci FY, Chang MH, Mah TS, Romero MF, Gorin MB (2006) Proximal renal tubular acidosis and ocular pathology: a novel missense mutation in the gene (SLC4A4) for sodium bicarbonate cotransporter protein (NBCe1). Mol Vis 12:324–330
8. Devonald MA, Smith AN, Poon JP, Ihrke G, Karet FE (2003) Non-polarized targeting of AE1 causes autosomal dominant distal renal tubular acidosis. Nat Genet 33:125–127
9. Dinour D, Chang MH, Satoh J, Smith BL, Angle N, Knecht A, Serban I, Holtzman EJ, Romero MF (2004) A novel missense mutation in the sodium bicarbonate cotransporter (NBCe1/SLC4A4) causes proximal tubular acidosis and glaucoma through ion transport defects. J Biol Chem 279:52238–52246

10. Disthabanchong S, Radinahamed P, Stitchantrakul W, Hongeng S, Rajatanavin R (2007) Chronic metabolic acidosis alters osteoblast differentiation from human mesenchymal stem cells. Kidney Int 71:201–209
11. Espiritu DJ, Bernardo AA, Arruda JA (2006) Role of NH_2 and COOH termini in targeting, stability, and activity of sodium bicarbonate cotransporter 1. Am J Physiol Renal Physiol 291:F588–F596
12. Gawenis LR, Bradford EM, Prasad V, Lorenz JN, Simpson JE, Clarke LL, Woo AL, Grisham C, Sanford LP, Doetschman T, Miller ML, Shull GE (2007) Colonic anion secretory defects and metabolic acidosis in mice lacking the NBC1 Na^+/HCO_3^- cotransporter. J Biol Chem 282:9042–9052
13. Horita S, Yamada H, Inatomi J, Moriyama N, Sekine T, Igarashi T, Endo Y, Dasouki M, Ekim M, Al-Gazali L, Shimadzu M, Seki G, Fujita T (2005) Functional analysis of NBC1 mutants associated with proximal renal tubular acidosis and ocular abnormalities. J Am Soc Nephrol 16:2270–2278
14. Igarashi T, Inatomi J, Sekine T, Cha SH, Kanai Y, Kunimi M, Tsukamoto K, Satoh H, Shimadzu M, Tozawa F, Mori T, Shiobara M, Seki G, Endou H (1999) Mutations in SLC4A4 cause permanent isolated proximal renal tubular acidosis with ocular abnormalities. Nat Genet 23:264–266
15. Igarashi T, Inatomi J, Sekine T, Seki G, Shimadzu M, Tozawa F, Takeshima Y, Takumi T, Takahashi T, Yoshikawa N, Nakamura H, Endou H (2001) Novel nonsense mutation in the Na^+/HCO_3^- cotransporter gene (SLC4A4) in a patient with permanent isolated proximal renal tubular acidosis and bilateral glaucoma. J Am Soc Nephrol 12:713–718
16. Inatomi J, Horita S, Braverman N, Sekine T, Yamada H, Suzuki Y, Kawahara K, Moriyama N, Kudo A, Kawakami H, Shimadzu M, Endou H, Fujita T, Seki G, Igarashi T (2004) Mutational and functional analysis of SLC4A4 in a patient with proximal renal tubular acidosis. Pflugers Arch 448:438–444
17. Ji W, Foo JN, O'Roak BJ, Zhao H, Larson MG, Simon DB, Newton-Cheh C, State MW, Levy D, Lifton RP (2008) Rare independent mutations in renal salt handling genes contribute to blood pressure variation. Nat Genet 40:592–599
18. Kao L, Sassani P, Azimov R, Pushkin A, Abuladze N, Peti-Peterdi J, Liu W, Newman D, Kurtz I (2008) Oligomeric structure and minimal functional unit of the electrogenic sodium bicarbonate cotransporter NBCe1-A. J Biol Chem 283:26782–26794
19. Li HC, Szigligeti P, Worrell RT, Matthews JB, Conforti L, Soleimani M (2005) Missense mutations in Na^+:HCO_3^- cotransporter NBC1 show abnormal trafficking in polarized kidney cells: a basis of proximal renal tubular acidosis. Am J Physiol Renal Physiol 289:F61–F71
20. Li HC, Li EY, Neumeier L, Conforti L, Soleimani M (2007) Identification of a novel signal in the cytoplasmic tail of the Na^+:HCO_3^- cotransporter NBC1 that mediates basolateral targeting. Am J Physiol Renal Physiol 292:F1245–F1255
21. Li HC, Kucher V, Li EY, Conforti L, Zahedi KA, Soleimani M (2012) The role of aspartic acid residues 405 and 416 of the kidney isotype of sodium-bicarbonate cotransporter 1 in its targeting to the plasma membrane. Am J Physiol Cell Physiol 302:C1713–C1730
22. Lo YF, Yang SS, Seki G, Yamada H, Horita S, Yamazaki O, Fujita T, Usui T, Tsai JD, Yu IS, Lin SW, Lin SH (2011) Severe metabolic acidosis causes early lethality in NBC1 W516X knock-in mice as a model of human isolated proximal renal tubular acidosis. Kidney Int 79:730–741
23. Marino CR, Jeanes V, Boron WF, Schmitt BM (1999) Expression and distribution of the Na^+–HCO_3^- cotransporter in human pancreas. Am J Physiol 277:G487–G494
24. Newman EA (1999) Sodium-bicarbonate cotransport in retinal astrocytes and Muller cells of the rat. Glia 26:302–308
25. Preisig PA, Alpern RJ (1989) Basolateral membrane H-OH-HCO_3 transport in the proximal tubule. Am J Physiol 256:F751–F765
26. Quilty JA, Cordat E, Reithmeier RA (2002) Impaired trafficking of human kidney anion exchanger (kAE1) caused by hetero-oligomer formation with a truncated mutant associated with distal renal tubular acidosis. Biochem J 368:895–903
27. Romero MF, Hediger MA, Boulpaep EL, Boron WF (1997) Expression cloning and characterization of a renal electrogenic Na^+/HCO_3^- cotransporter. Nature 387:409–413
28. Romero MF, Boron WF (1999) Electrogenic Na^+/HCO_3^- cotransporters: cloning and physiology. Annu Rev Physiol 61:699–723
29. Schmitt BM, Berger UV, Douglas RM, Bevensee MO, Hediger MA, Haddad GG, Boron WF (2000) Na/HCO_3 cotransporters in rat brain: expression in glia, neurons, and choroid plexus. J Neurosci 20:6839–6848
30. Shiohara M, Igarashi T, Mori T, Komiyama A (2000) Genetic and long-term data on a patient with permanent isolated proximal renal tubular acidosis. Eur J Pediatr 159:892–894
31. Shirakabe K, Priori G, Yamada H, Ando H, Horita S, Fujita T, Fujimoto I, Mizutani A, Seki G, Mikoshiba K (2006) IRBIT, an inositol 1,4,5-trisphosphate receptor-binding protein, specifically binds to and activates pancreas-type Na^+/HCO_3^- cotransporter 1 (pNBC1). Proc Natl Acad Sci U S A 103:9542–9547
32. Suzuki M, Vaisbich MH, Yamada H, Horita S, Li Y, Sekine T, Moriyama N, Igarashi T, Endo Y, Cardoso TP, de Sa LC, Koch VH, Seki G, Fujita T (2008) Functional analysis of a novel missense NBC1 mutation and of other mutations causing proximal renal tubular acidosis. Pflugers Arch 455:583–593
33. Suzuki M, Van Paesschen W, Stalmans I, Horita S, Yamada H, Bergmans BA, Legius E, Riant F, De Jonghe P, Li Y, Sekine T, Igarashi T, Fujimoto I, Mikoshiba K, Shimadzu M, Shiohara M, Braverman N, Al-Gazali L, Fujita T, Seki G (2010) Defective membrane expression of the Na^+–HCO_3^- cotransporter NBCe1 is associated with familial migraine. Proc Natl Acad Sci U S A 107:15963–15968
34. Svichar N, Esquenazi S, Chen HY, Chesler M (2011) Preemptive regulation of intracellular pH in hippocampal neurons by a dual mechanism of depolarization-induced alkalinization. J Neurosci 31:6997–7004
35. Terada N, Ohno N, Saitoh S, Seki G, Komada M, Suzuki T, Yamakawa H, Soleimani M, Ohno S (2007) Interaction of membrane skeletal protein, protein 4.1B and p55, and sodium bicarbonate cotransporter1 in mouse renal S1–S2 proximal tubules. J Histochem Cytochem 55:1199–1206
36. Toye AM, Parker MD, Daly CM, Lu J, Virkki LV, Pelletier MF, Boron WF (2006) The human NBCe1-A mutant R881C, associated with proximal renal tubular acidosis, retains function but is mistargeted in polarized renal epithelia. Am J Physiol Cell Physiol 291:C788–C801
37. Usui T, Hara M, Satoh H, Moriyama N, Kagaya H, Amano S, Oshika T, Ishii Y, Ibaraki N, Hara C, Kunimi M, Noiri E, Tsukamoto K, Inatomi J, Kawakami H, Endou H, Igarashi T, Goto A, Fujita T, Araie M, Seki G (2001) Molecular basis of ocular abnormalities associated with proximal renal tubular acidosis. J Clin Invest 108:107–115
38. Yamada H, Yamazaki S, Moriyama N, Hara C, Horita S, Enomoto Y, Kudo A, Kawakami H, Tanaka Y, Fujita T, Seki G (2003) Localization of NBC-1 variants in human kidney and renal cell carcinoma. Biochem Biophys Res Commun 310:1213–1218
39. Yamazaki O, Yamada H, Suzuki M, Horita S, Shirai A, Nakamura M, Seki G, Fujita T (2011) Functional characterization of nonsynonymous single nucleotide polymorphisms in the electrogenic Na^+–HCO_3^- cotransporter NBCe1A. Pflugers Arch 461:249–259
40. Zhu Q, Kao L, Azimov R, Newman D, Liu W, Pushkin A, Abuladze N, Kurtz I (2010) Topological location and structural importance of the NBCe1-A residues mutated in proximal renal tubular acidosis. J Biol Chem 285:13416–13426